1 **ATP release from influenza-infected lungs enhances neutrophil activation and promotes**

2 **disease progression**

3

4 Carola Ledderose[1,2], Eleftheria-Angeliki Valsami[2], Mark Elevado[2], Wolfgang G. Junger[1,2]

5

6 [1]Department of Surgery, University of California, San Diego Health, San Diego, CA, USA

7 [2]Department of Surgery, Beth Israel Deaconess Medical Center, Harvard Medical School,

8 Boston, MA, USA

9

10 Correspondence address: Wolfgang G. Junger, UC San Diego Health, Department of Surgery,

11 9452 Medical Center Drive, La Jolla, CA 92037, USA; e-mail: wgjunger@health.ucsd.edu

12

13 **Running Title:** Influenza primes neutrophils via ATP

14 **Word count (Background to end of Discussion):** 3299

15 **Word count (Abstract):** 198

16

17 **Summary**

18 Influenza infection releases ATP that primes peripheral neutrophils and causes their excessive

19 activation after they infiltrate the lungs. Thus, ATP-induced neutrophil priming may be a

20 therapeutic target to reduce lung tissue damage in severe influenza cases.

21

ABSTRACT

Background: ATP enhances neutrophil responses, but little is known about the role of ATP in influenza infections.

Methods: We used a mouse influenza model to study if ATP release is associated with neutrophil activation and disease progression.

Results: Influenza infection increased pulmonary ATP levels 5-fold and plasma ATP levels 3-fold over the levels in healthy mice. Adding ATP at those concentrations to blood from healthy mice primed their neutrophils and enhanced CD11b and CD63 expression, CD62L shedding, and reactive oxygen species production in response to formyl peptide receptor (FPR) stimulation. Influenza infection also primed neutrophils *in vivo*, resulting in FPR-induced CD11b expression and CD62L shedding up to 3-times higher than that of uninfected mice. In infected mice, large numbers of neutrophils entered the lungs. These cells were significantly more activated than peripheral neutrophils of infected and pulmonary neutrophils of healthy mice. Plasma ATP levels of infected mice and influenza disease progression corresponded with the numbers and activation level of their pulmonary neutrophils.

Conclusion: Our findings suggest that ATP release from the lungs of infected mice promotes influenza disease progression by priming peripheral neutrophils that become strongly activated and cause pulmonary tissue damage after their recruitment to the lungs.

41 **Key words**: influenza, mice, neutrophil priming and activation, purinergic signaling, ATP

42 release

43

BACKGROUND

45 Influenza is one of the most widespread respiratory viral diseases [1]. It is associated with

46 significant morbidity and mortality and causes over 5 million hospitalizations and approximately

47 300,000 deaths worldwide each year [2, 3]. Influenza is particularly fatal in infants, older people,

48 and in patients with chronic pulmonary diseases and other comorbidities [3, 4]. Highly

49 pathogenic and pandemic influenza A virus strains can cause lethal illness even among less

50 vulnerable adult populations [5]. Severe disease often involves a dysregulated immune response

51 that results in pneumonia, acute respiratory distress syndrome (ARDS), and multiple organ

52 dysfunction syndrome (MODS) [6, 7].

53

54 The role of polymorphonuclear neutrophils (PMNs) in influenza infections is not clear [8-10].

55 Some studies have shown that PMNs reduce viral spread, help to resolve inflammation, and

56 prevent secondary bacterial infections that often complicate the treatment of severe influenza

57 cases [9, 11, 12]. Other reports suggest that PMNs contribute to excessive inflammation that

58 promotes pulmonary tissue damage and disease progression following influenza virus infections

59 [13-15].

60

61 PMNs are essential for antimicrobial host defense. They rapidly accumulate in the circulation

62 and infiltrate sites of infection by attaching to the endothelial layer of blood vessels and

63 transmigrating into affected tissues. These processes require the upregulation of CD11b on the

64   cell surface of PMNs and shedding of CD62L (L-selectin) [16, 17]. At the sites of infection,

65   chemotaxis guides PMNs towards microbial invaders that they entrap and kill with a wide

66   arsenal of defensive strategies [18, 19].

67

68   Gradient sensing and chemotaxis of PMNs towards bacterial invaders depend on cellular ATP

69   release and autocrine feedback mechanisms that involve purinergic receptors [20]. The family of

70   purinergic receptors comprises seven P2X, eight P2Y, and four P1 receptors that recognize ATP,

71   ADP, adenosine, and related nucleotides [21]. PMNs express primarily the P2Y2 and A2a

72   subtypes [22]. ATP promotes PMN responses via P2Y2 receptors, while the ATP breakdown

73   product adenosine attenuates cell responses via A2a receptor signaling. The orchestrated actions

74   of both purinergic receptor subtypes regulate complex PMN functions including gradient

75   sensing, chemotaxis, and the phagocytosis of invading microorganisms [20, 22, 23].

76

77   However, damaged host tissues also release ATP, which acts as a danger signal that promotes

78   inflammation and alters immune responses [24]. High extracellular ATP levels not only disrupt

79   the regulatory mechanisms that PMNs need for host defense [23, 25] but also promote the

80   uncontrolled production and release of cytotoxic mediators that further damage alveolar

81   epithelial-endothelial barriers and contribute to ARDS and MODS [7, 10].

82

83   Several studies have shown that viral infections cause ATP release. For example, infections with

84   human immunodeficiency virus, severe acute respiratory syndrome coronavirus 2, vesicular

85   stomatitis virus, and certain influenza virus strains have been shown to cause ATP release that is

86   thought to affect viral entry, viral replication, and inflammation [26-29]. In this study, we

87 evaluated the hypothesis that influenza infection-induced ATP release contributes to disease

88 progression by promoting dysregulated PMN activation that damages lung tissues.

89

90 **MATERIALS AND METHODS**

91 **Virus preparation**

92 The mouse-adapted influenza virus strain (H1N1) A/Puerto Rico/8-9NMC3/1934 (PR8) was

93 from the BEI Resources Repository (NR-29025; National Institute of Allergy and Infectious

94 Diseases) and kindly provided by Dr. Daniel Lingwood (Ragon Institute, Massachusetts General

95 Hospital, Boston, MA). Virus stocks were propagated in Madin-Darby Canine Kidney (MDCK)

96 cells (ATCC, Manassas, VA), titrated, and their concentrations shown as median tissue culture

97 infectious doses ($TCID_{50}$) following previously described protocols [30].

98

99 **Mice**

100 All animal experiments were approved by the Institutional Animal Care and Use Committee of

101 Beth Israel Deaconess Medical Center and performed in accordance with National Institutes of

102 Health guidelines for the care and use of laboratory animals. C57BL/6J mice were from Jackson

103 Laboratory (Bar Harbor, ME), housed in groups of 2-5 mice per cage with free access to standard

104 rodent food and water, and maintained at a 12-hour dark/light cycle. Experiments were

105 performed with equal numbers of 8- to 12-week-old male and female mice per group.

106

107 **Influenza infection model**

108 Mice were lightly anesthetized with isoflurane and intranasally infected with indicated doses of

109 influenza virus preparations in sterile phosphate buffered saline (PBS) using 20 µl per nostril.

110   Control animals received equal volumes of PBS. Buprenorphine SR-LAB (1.2 mg/kg;

111   ZooPharm, Laramie, WY) administered subcutaneously at the time of infection was used for

112   pain control. Animals were assessed at least twice daily and clinical signs of illness and body

113   weight were recorded.

114

115   **Blood collection**

116   At indicated time points, mice were anesthetized and exsanguinated by cardiac puncture. Blood

117   was drawn from the right ventricle using a 23-gauge needle and a 1-ml syringe wetted with

118   sodium heparin. For the analysis of plasma ATP concentrations, aliquots of blood were

119   immediately chilled in an ice water bath. The remaining blood was kept at room temperature and

120   analyzed by flow cytometry within 1 h after blood collection.

121

122   **Analysis of plasma ATP levels with high performance liquid chromatography (HPLC)**

123   Plasma ATP concentrations were determined as previously described [31]. Briefly, plasma was

124   prepared from chilled heparinized blood samples, stabilized with perchloric acid

125   (MilliporeSigma, St. Louis, MO), and spiked with the internal standard adenosine 5'-(α,β-

126   methylene)-diphosphate (AMPCP; MilliporeSigma). Fluorescent 1,N^6-etheno-derivatives of ATP

127   and AMPCP were generated, pre-purified by solid phase extraction, and concentrated as

128   described [31]. Samples were analyzed with an Agilent 1260 Infinity HPLC system (Agilent,

129   Santa Clara, CA). Plasma ATP concentrations were calculated based on a standard mixture of

130   ATP and AMPCP processed and analyzed in parallel.

131

132   **PMN blood counts**

133 Heparinized blood samples were labeled with anti-CD11b APC (clone M1/70) and anti-Ly6G

134 Brilliant Violet 421 (clone 1A8) antibodies (BioLegend, San Diego, CA) for 20 min on ice,

135 treated with RBC Lysis/Fixation buffer (BioLegend), and the numbers of PMNs (CD11b/Ly6G

136 double-positive cells) were determined by flow cytometry (NovoCyte 3000, Agilent, Santa

137 Clara, CA).

138

Assessment of PMN activation levels

140 CD11b expression and CD62L shedding were measured to assess PMN activation states.

141 Heparinized blood samples were stained with anti-Ly6G Brilliant Violet 421, anti-CD11b APC,

142 and anti-CD62L FITC (clone MEL-14) antibodies (BioLegend), treated with RBC Lysis/Fixation

143 buffer, and analyzed by flow cytometry. Fluorescence-minus-one controls (FMO) were used to

144 define positive staining. CD11b positive (CD11b$^+$) PMNs were defined as PMNs displaying

145 CD11b fluorescence higher than unstimulated PMNs of healthy controls.

146

Assessing the priming state of PMNs

148 Priming of PMNs exposed to different concentrations of ATP or viral infection was assessed by

149 measuring their response to *in vitro* stimulation with the formyl peptide receptor (FPR) agonist

150 WKYMVm (W-peptide; Tocris Bioscience, Minneapolis, MN) compared to unprimed cells.

151 Specifically, we analyzed shedding of CD62L, the upregulation of CD11b or the degranulation

152 marker CD63, and the production of reactive oxygen species (ROS) as previously described [32].

153 Blood from healthy mice was treated for 1 min with ATP (MilliporeSigma). Then, these samples

154 or blood from virus-infected mice were stimulated with 50 nM W-peptide for 10 min at 37°C.

155 For the assessment of ROS production, blood samples were stained for 5 min with 100 µM

156   dihydrorhodamine-123 (DHR; Invitrogen, Carlsbad, CA), treated or not with ATP, and

157   stimulated with 100 nM W-peptide for 20 min. The reactions were stopped on ice, samples

158   stained with anti-Ly6G Brilliant Violet 421, anti-CD11b APC, anti-CD62L FITC, and anti-CD63

159   PE (clone NVG-2, BioLegend) antibodies, treated with RBC Lysis/Fixation buffer, and analyzed

160   by flow cytometry.

161

162   **Analysis of PMN numbers in bronchoalveolar lavage fluids**

163   Immediately after exsanguination, a blunt 23-gauge needle was inserted into the trachea and

164   bronchoalveolar lavage fluid (BALF) was collected by flushing the lungs four times each with

165   1 ml ice-cold lavage fluid. The first lavage was done with sterile saline followed by three

166   additional lavages with saline containing 0.1% bovine serum albumin (BSA). BALF samples

167   were centrifuged at 400 x g for 5 min at 0°C. The supernatant of the first lavage was treated with

168   perchloric acid and stored at -80°C for HPLC analysis. Cell pellets from the combined lavage

169   fluids were used to assess total leukocyte counts with a hemocytometer. For differential counting

170   of leukocytes, cells were stained with a Hema 3^{TM} staining kit (Fisher Scientific, Waltham, MA)

171   and 200 cells per sample were analyzed.

172

173   **Analysis of PMN activation in the lungs**

174   CD11b expression levels of PMNs in BALF samples were determined as a measure of the

175   activation of PMNs recruited into the lungs. BALF samples were adjusted to a cell concentration

176   of 5-10 x 10^5 cells/ml, stained with anti-CD11b and anti-Ly6G antibodies, washed with PBS/1%

177   BSA, and analyzed by flow cytometry. PMNs were identified as cells that are positive for

178   CD11b and Ly6G. Cellular debris was analyzed based on forward and side scatter properties and

179   CD11b and Ly6G staining to estimate the degree of PMN deterioration following degranulation.

180

181   **Analysis of ATP levels in bronchoalveolar lavage fluids**

182   BALF samples stabilized with perchloric acid and stored at -80°C were thawed on ice, spiked

183   with AMPCP, and analyzed by HPLC as described above. Alveolar ATP concentrations were

184   estimated based on the approximate alveolar fluid lining volume of 6 µl reported for mouse lungs

185   [33].

186

187   **Statistical analyses**

188   Differences between two groups were tested for statistical significance using a two-tailed t test or

189   Mann-Whitney test for normally and not normally distributed data, respectively. One-way

190   ANOVA followed by Holm-Sidak's test was used for multiple group comparisons when data

191   were normally distributed. Kruskal-Wallis and post-hoc Dunn's tests were used when data were

192   not normally distributed. Correlations between parameters were assessed by Pearson's test. Four-

193   parameter logistic regression curve fittings and calculations of half maximal effective

194   concentrations (EC_{50}) as well as all other statistical analyses were done with SigmaPlot 12.5

195   software (Systat Software Inc., San Jose, CA). Differences were considered statistically

196   significant at $p < 0.05$.

197

198   **RESULTS**

199   **Influenza infection of mice causes PMN accumulation in the lungs**

200   Infection of mice with the mouse-adapted influenza A virus strain PR8 at a dose of 500 $TCID_{50}$

201 or higher led to a significant body weight loss within 3 days (Figure 1A). Significant weight loss

202 was evident within 2 days after infection with a dose of 1,000 TCID$_{50}$, resulting in an average

203 drop in body weight of about 20% within 4 days (Figure 1B). This dose also caused a 10-fold

204 increase in the number of leukocytes in the BALF 3 days after infection. The numbers of PMNs

205 rose from about 80 cells in control animals to 1.4 x 10^6 cells in infected mice (Figure 1C). In

206 addition, the average number of PMNs in blood nearly doubled from 140 ± 22 per µl in controls

207 to 266 ± 37 per µl in infected animals (Figure 1C). These results are consistent with previous

208 reports that PMN influx into the lungs contributes to the pathogenesis of influenza [13, 14, 34].

209

210 **ATP release correlates with disease progression**

211 Next, we studied whether influenza infection alters extracellular ATP levels. Mice were infected

212 with 500-1,500 TCID$_{50}$ of PR8 virus and plasma ATP concentrations were determined 3 days

213 later. We found dose-dependent increases in plasma ATP levels (Figure 2A). At the highest viral

214 load, plasma ATP levels reached an average of about 170 nM, which was 3-times higher than in

215 healthy controls. ATP concentrations in moderately sick animals doubled from a baseline value

216 of 60 ± 7 nM to 128 ± 15 nM 3 days after infection (Figure 2B). ATP levels correlated with body

217 weight loss (Figure 2C), which is a reliable indicator of disease progression in influenza-infected

218 mice [35]. In summary, these data show that ATP release is associated with influenza infection

219 and disease progression.

220

221 **ATP released in the lungs of influenza-infected mice spreads throughout their circulation**

222 A source of ATP in the plasma of infected mice is the release from damaged tissue in the lungs.

223 As shown in Figure 3A, lung ATP levels 3 days after infection with 1,000 TCID$_{50}$ were with

224   5,650 ± 880 nM over 5-times higher than in healthy controls (1,020 ± 250 nM). ATP plasma

225   levels in these animals were about 3-times higher (156 ± 14 nM) when compared to healthy mice

226   (59 ± 7 nM; Figure 3A). The ATP concentrations in the alveolar space correlated significantly

227   with plasma ATP levels (Figure 3B), suggesting that ATP leaking from damaged lung tissue

228   spreads throughout the circulatory system of infected mice.

229

230   **Extracellular ATP dose-dependently primes mouse PMNs**

231   The transition of PMNs from a quiescent to a fully activated state involves PMN priming, which

232   readies PMNs for robust functional responses to a variety of subsequent stimuli [36].

233   Extracellular ATP is known to prime human PMN responses to formyl peptide receptor (FPR)

234   stimulation [37, 38]. We studied whether ATP has similar priming effects on mouse PMNs.

235   Adding ATP to blood samples of healthy mice dose-dependently augmented CD11b expression

236   on the surface of PMNs in response to FPR stimulation with the agonist W-peptide (Figure 4A).

237   ATP levels as low as 100 nM primed CD11b responses by about 15-fold with an EC_{50} value of

238   140 nM ATP (Figure 4A-B). ATP also markedly increased the shedding of CD62L in response

239   to FPR stimulation with an EC_{50} value of 114 nM (Figure 4C-D). CD11b expression and CD62L

240   shedding are both early and sensitive markers of PMN activation and aid the transendothelial

241   migration of PMNs to sites of infection [16, 17]. ATP also primed PMN degranulation and

242   oxidative burst as seen by increased CD63 expression and ROS production (Supplementary

243   Figure 1).

244

245   **Influenza infection primes circulating PMNs**

246   Taken together, the findings above suggest that the increase in extracellular ATP enhances the

247 priming state of PMNs following influenza infection. Indeed, we found that PMNs of influenza-

248 infected mice showed significantly stronger CD11b expression responses to FPR stimulation

249 when compared to healthy controls (Figure 5A). Similarly, FPR-induced CD62L shedding was

250 significantly higher when compared to PMNs of healthy mice (Figure 5B). These priming effects

251 on PMNs gradually increased over time after viral infection (Figure 5C-D). Taken together with

252 the time-dependent increase in plasma ATP levels in infected mice (Figure 2B) and the priming

253 effect of ATP on mouse PMNs (Figure 4), these results suggest that ATP that is released from

254 damaged lungs drives PMN priming in influenza-infected mice.

255

256 **PMNs are activated in the lungs but not in the circulation of influenza-infected mice**

257 As shown above, influenza caused a robust increase in the priming state of peripheral PMNs,

258 making them significantly more responsive to FPR stimulation (Figure 5). However, the

259 activation state of PMNs in the blood was not markedly increased and CD11b expression did not

260 differ between infected and healthy animals (Figure 6A). The same was true for CD62L

261 shedding (Figure 5B). However, the PMNs that infiltrated the lungs of infected mice showed

262 strong CD11b expression, which was significantly higher than that of peripheral PMNs and of

263 PMNs in the lungs of healthy mice (Figure 6B). Taken together, these findings show that

264 influenza infection primes peripheral PMNs, but that these cells become activated only after their

265 recruitment into the lungs, possibly by local release of mediators that stimulate FPR or other

266 danger-sensing receptors of PMNs.

267

268 **Activation of pulmonary PMNs correlates with disease progression**

269 Activated PMNs degranulate and release their arsenal of cytotoxic mediators to kill invading

270   microorganisms but this can also cause substantial collateral damage to host tissues [39]. We

271   found that the percentage of PMNs infiltrating the lungs correlated with body weight loss of

272   influenza-infected mice (Figure 7A). In addition, expression levels of the PMN activation marker

273   CD11b on cellular debris found in the lungs of infected animals closely correlated with body

274   weight loss, suggesting that PMN degranulation promotes disease progression (Figure 7B).

275   Furthermore, high CD11b expression levels on Ly6G-positive cellular debris derived from

276   PMNs correlated with increased plasma ATP concentrations (Figure 7C). Taken together, these

277   findings suggest that the peripheral priming of PMNs by ATP followed by their influx and

278   activation in the lungs leads to PMN degranulation that damages lung tissue and defines disease

279   progression in influenza virus infection (Figure 7D).

280

281   **DISCUSSION**

282   Influenza remains a leading cause of morbidity and mortality worldwide [2]. In severe influenza

283   cases, a so-called "cytokine storm," inflammatory tissue damage, and secondary microbial

284   infections culminate in lethal complications such as pneumonia, ARDS, sepsis, and MODS [6,

285   7]. PMNs are among the first immune cells recruited into influenza-infected lungs where they are

286   thought to fight microbial invaders. However, when dysregulated, PMNs lose their ability to

287   locate and eliminate invading microbes and instead contribute to lung tissue damage through

288   uncontrolled release of ROS, proteinases, and other cytotoxic mediators [10, 13, 15].

289

290   We found increased numbers of PMNs in the circulation and the lungs of influenza-infected

291   mice, which was paralleled by an increase in extracellular ATP levels in the alveolar space and

292   plasma. PMNs themselves release ATP to regulate chemotaxis and other defensive effector

293   functions via complex autocrine feedback mechanisms that involve P2Y2 and adenosine A2a

294   receptors on the cell surface [20, 22, 23, 40, 41]. Uncontrolled accumulation of ATP in the

295   extracellular environment distorts these autocrine feedback mechanisms, resulting in impaired

296   antimicrobial host defenses and uncontrolled release of cytotoxic mediators that cause collateral

297   tissue damage [37, 42, 43].

298

299   The accumulation of PMN debris we found in the lungs of infected mice suggests that PMN-

300   mediated lung tissue damage is a main source of the increased extracellular ATP levels in our

301   influenza model. However, other mechanisms may also contribute to the accumulation of

302   extracellular ATP. For example, NLPR3 inflammasome activation involves ATP release and

303   P2X7 receptor stimulation. Previous work has shown reduced PMN infiltration and improved

304   survival of influenza-infected P2X7 receptor-deficient mice when compared to wild-type mice,

305   which supports the notion that NLPR3 inflammasome/P2X7 receptor signaling contributes to

306   PMN dysregulation and influenza disease progression [44].

307

308   We found that extracellular ATP concentrations as low as 100 nM were sufficient to prime

309   mouse PMNs and that equivalent ATP levels were readily achieved in the alveolar and plasma

310   compartments of influenza-infected mice. Although circulating PMNs of these mice were

311   strongly primed, only PMNs in the lungs were activated. However, the primed state of the

312   circulating PMNs resulted in significantly enhanced cell activation in response to stimulation

313   with the FPR agonist W-peptide. The primed state of peripheral PMNs increased over time after

314   influenza infection and paralleled the increase in plasma ATP levels. The observation that PMNs

315   are activated only after their recruitment into the lungs indicates that additional stimuli in

316   infected lungs complete the stimulation process that results in full PMN activation. This concept

317   is supported by previous work that has shown that ATP primes PMNs but does not activate these

318   cells in the absence of other stimuli [37, 38].

319

320   The activation of PMNs in the lungs of influenza-infected mice may occur through local stimuli

321   such as pathogen- or danger-associated molecular patterns (PAMPs and DAMPs), which include

322   ligands of Toll-like (TLR), NOD-like (NLR), and formyl peptide receptors (FPR) that are

323   released in inflamed and infected tissues [45, 46]. Along with released ATP, those PAMPs and

324   DAMPs may lead to uncontrolled PMN activation, driving a feed-forward process that

325   culminates in disease progression and the lethal consequences of severe cases of influenza

326   infections (Figure 7D).

327

328   Our findings suggest that extracellular ATP accumulation could be a potential therapeutic target

329   to treat severe influenza cases. Possible therapeutic strategies could include treatments with

330   antagonists of P2Y2 and P2X7 receptors, with ATP-hydrolyzing enzymes such as apyrase, or

331   with other drugs that target ATP release mechanisms [44, 47]. These approaches have yielded

332   encouraging results in mouse models of influenza and other clinical conditions that culminate in

333   ARDS and MODS, including endotoxemia, pancreatitis, and sepsis [25, 47-50].

334

335   A limitation of our study is that the mouse model we used does not fully replicate typical human

336   influenza cases, but rather infections with highly pathogenic influenza strains, which often

337   include secondary bacterial infections [12]. Therapeutic strategies such as the ones mentioned

338   above will be complicated by the fact that removal of extracellular ATP can impair antimicrobial

host defenses, e.g., PMN gradient sensing and chemotaxis that require autocrine purinergic

signaling. Effective therapeutic interventions targeting ATP must find a balance between the

dual roles of ATP as a regulator and disruptor of PMN functions. Future work will have to

evaluate the potential of ATP and purinergic signaling mechanisms as viable therapeutic targets

to improve outcome in clinically relevant models of influenza infections.

REFERENCES

1. Paules C, Subbarao K. Influenza. Lancet **2017**; 390:697-708.

2. Lafond KE, Porter RM, Whaley MJ, et al. Global burden of influenza-associated lower respiratory tract infections and hospitalizations among adults: A systematic review and meta-analysis. PLoS Med **2021**; 18(3):e1003550.

3. Uyeki TM, Hui DS, Zambon M, Wentworth DE, Monto AS. Influenza. Lancet **2022**; 400:693-706.

4. Kunisaki KM, Janoff EN. Influenza in immunosuppressed populations: a review of infection frequency, morbidity, mortality, and vaccine responses. Lancet Infect Dis **2009**; 9:493-504.

362   5. Taubenberger JK, Morens DM. The pathology of influenza virus infections. Annu Rev
363   Pathol **2008**; 3:499-522.

364   6. de Jong MD, Simmons CP, Thanh TT, et al. Fatal outcome of human influenza A (H5N1)
365   is associated with high viral load and hypercytokinemia. Nat Med **2006**; 12:1203-07.

366   7. Short KR, Kroeze EJBV, Fouchier RAM, Kuiken T. Pathogenesis of influenza-induced
367   acute respiratory distress syndrome. Lancet Infect Dis **2014**; 14:57-69.

368   8. Tumpey TM, García-Sastre A, Taubenberger JK, et al. Pathogenicity of influenza viruses
369   with genes from the 1918 pandemic virus: functional roles of alveolar macrophages and
370   neutrophils in limiting virus replication and mortality in mice. J Virol **2005**; 79:14933-44.

371   9. Tate MD, Deng YM, Jones JE, Anderson GP, Brooks AG, Reading PC. Neutrophils
372   ameliorate lung injury and the development of severe disease during influenza infection.
373   J Immunol **2009**; 183:7441-50.

374   10. Narasaraju T, Yang E, Samy RP, et al. Excessive neutrophils and neutrophil extracellular
375   traps contribute to acute lung injury of influenza pneumonitis. Am J Pathol **2011**;
376   179:199-210.

377   11. Tate MD, Ioannidis LJ, Croker B, Brown LE, Brooks AG, Reading PC. The role of
378   neutrophils during mild and severe influenza virus infections of mice. PLoS One **2011**;
379   6(3):e17618.

380   12. Morens DM, Taubenberger JK, Fauci AS. Predominant role of bacterial pneumonia as a
381   cause of death in pandemic influenza: implications for pandemic influenza preparedness.
382   J Infect Dis **2008**; 198:962-70.

383   13. Perrone LA, Plowden JK, García-Sastre A, Katz JM, Tumpey TM. H5N1 and 1918

384   pandemic influenza virus infection results in early and excessive infiltration of

385   macrophages and neutrophils in the lungs of mice. PLoS Pathog **2008**; 4(8):e1000115.

386   14. Dunning J, Blankley S, Hoang LT, et al. Progression of whole-blood transcriptional

387   signatures from interferon-induced to neutrophil-associated patterns in severe influenza.

388   Nat Immunol **2018**; 19:625-35.

389   15. Tang BM, Shojaei M, Teoh S, et al. Neutrophils-related host factors associated with

390   severe disease and fatality in patients with influenza infection. Nat Commun **2019**;

391   10:3422.

392   16. Rochon YP, Kavanagh TJ, Harlan JM. Analysis of integrin (CD11b/CD18) movement

393   during neutrophil adhesion and migration on endothelial cells. J Microsc **2000**; 197:15-

394   24.

395   17. Rahman I, Collado Sánchez A, Davies J, et al. L-selectin regulates human neutrophil

396   transendothelial migration. J Cell Sci **2021**; 134:jcs250340.

397   18. Winterbourn CC, Kettle AJ, Hampton MB. Reactive oxygen species and neutrophil

398   function. Annu Rev Biochem **2016**; 85:765-92.

399   19. Othman A, Sekheri M, Filep JG. Roles of neutrophil granule proteins in orchestrating

400   inflammation and immunity. FEBS J **2022**; 289:3932-53.

401   20. Junger WG. Immune cell regulation by autocrine purinergic signalling. Nat Rev Immunol

402   **2011**; 11:201-12.

403   21. Ralevic V, Burnstock G. Receptors for purines and pyrimidines. Pharmacol Rev **1998**;

404   50:413-92.

405   22. Bao Y, Chen Y, Ledderose C, Li L, Junger WG. Pannexin 1 channels link

406   chemoattractant receptor signaling to local excitation and global inhibition responses at

407   the front and back of polarized neutrophils. J Biol Chem **2013**; 288:22650-57.

408   23. Chen Y, Corriden R, Inoue Y, et al. ATP release guides neutrophil chemotaxis via P2Y2

409   and A3 receptors. Science **2006**; 314:1792-95.

410   24. Idzko M, Ferrari D, Eltzschig HK. Nucleotide signalling during inflammation. Nature

411   **2014**; 509:310-17.

412   25. Li X, Kondo Y, Bao Y, et al. Systemic adenosine triphosphate impairs neutrophil

413   chemotaxis and host defense in sepsis. Crit Care Med **2017**; 45:e97-e104.

414   26. Velasquez S, Prevedel L, Valdebenito S, et al. Circulating levels of ATP is a biomarker

415   of HIV cognitive impairment. EBioMedicine **2020**; 51:102503.

416   27. da Silva GB, Manica D, da Silva AP, et al. High levels of extracellular ATP lead to

417   different inflammatory responses in COVID-19 patients according to the severity. J Mol

418   Med (Berl) **2022**; 100:645-63.

419   28. Zhang C, He H, Wang L, et al. Virus-triggered ATP release limits viral replication

420   through facilitating IFN-β production in a P2X7-dependent manner. J Immunol 2017;

421   199:1372-81.

422   29. Wolk KE, Lazarowski ER, Traylor ZP, et al. Influenza A virus inhibits alveolar fluid

423   clearance in BALB/c mice. Am J Respir Crit Care Med **2008**; 178:969-76.

424   30. Karakus U, Crameri M, Lanz C, Yángüez E. Propagation and titration of influenza

425   viruses. Methods Mol Biol **2018**; 1836:59-88.

426   31. Ledderose C, Valsami EA, Junger WG. Optimized HPLC method to elucidate the

427   complex purinergic signaling dynamics that regulate ATP, ADP, AMP, and adenosine

428   levels in human blood. Purinergic Signal **2022**; 18:223-39.

429   32. Ledderose C, Hashiguchi N, Valsami EA, Rusu C, Junger WG. Optimized flow

430   cytometry assays to monitor neutrophil activation in human and mouse whole blood

431   samples. J Immunol Methods **2023**; 512:113403.

432   33. Icard P, Saumon G. Alveolar sodium and liquid transport in mice. Am J Physiol **1999**;

433   277: L1232-L8.

434   34. Brandes M, Klauschen F, Kuchen S, Germain RN. A systems analysis identifies a

435   feedforward inflammatory circuit leading to lethal influenza infection. Cell **2013**;

436   154:197-212.

437   35. Trammell RA, Toth LA. Markers for predicting death as an outcome for mice used in

438   infectious disease research. Comp Med **2011**; 61:492-8.

439   36. Condliffe AM, Kitchen E, Chilvers ER. Neutrophil priming: pathophysiological

440   consequences and underlying mechanisms. Clin Sci (Lond) **1998**; 94:461-71.

441   37. Kuhns DB, Wright DG, Nath J, Kaplan SS, Basford RE. ATP induces transient elevations

442   of $[Ca^{2+}]_i$ in human neutrophils and primes these cells for enhanced O_2^- generation. Lab

443   Invest **1988**; 58:448-53.

444   38. Ledderose C, Valsami EA, Newhams M, Elevado MJ, Novak T, Randolph AG, Junger

445   WG. ATP breakdown in plasma of children limits the antimicrobial effectiveness of their

446   neutrophils. Purinergic Signal **2023**; doi: 10.1007/s11302-022-09915-w. [online ahead of

447   print]

448   39. Kruger P, Saffarzadeh M, Weber AN, et al. Neutrophils: Between host defence, immune

449   modulation, and tissue injury. PLoS Pathog **2015**; 11(3),e1004651.

450   40. Chen Y, Yao Y, Sumi Y, et al. Purinergic signaling: a fundamental mechanism in

451   neutrophil activation. Sci Signal **2010**; 3(125):ra45.

452   41. Wang X, Chen D. Purinergic regulation of neutrophil function. Front Immunol **2018**;

453   9:399.

454   42. Seifert R, Wenzel K, Eckstein F, Schultz G. Purine and pyrimidine nucleotides potentiate

455   activation of NADPH oxidase and degranulation by chemotactic peptides and induce

456   aggregation of human neutrophils via G proteins. Eur J Biochem **1989**; 181:277-85.

457   43. Axtell RA, Sandborg RR, Smolen JE, Ward PA, Boxer LA. Exposure of human

458   neutrophils to exogenous nucleotides causes elevation in intracellular calcium,

459   transmembrane calcium fluxes, and an alteration of a cytosolic factor resulting in

460   enhanced superoxide production in response to FMLP and arachidonic acid. Blood **1990**;

461   75:1324‑32.

462   44. Leyva-Grado VH, Ermler ME, Schotsaert M, Gonzalez MG, Gillespie V, Lim JK,

463   García-Sastre A. Contribution of the purinergic receptor P2X7 to development of lung

464   immunopathology during influenza virus infection. mBio **2017**; 8:e00229-17.

465   45. Zhang Q, Raoof M, Chen Y, et al. Circulating mitochondrial DAMPs cause inflammatory

466   responses to injury. Nature **2010**; 464:104-7.

467   46. Iwasaki A, Pillai PS. Innate immunity to influenza virus infection. Nat Rev Immunol

468   **2014**; 14:315-28.

469   47. Reutershan J, Vollmer I, Stark S, Wagner R, Ngamsri KC, Eltzschig HK. Adenosine and

470   inflammation: CD39 and CD73 are critical mediators in LPS-induced PMN trafficking

471   into the lungs. FASEB J **2009**; 23:473-82.

472   48. Dixit A, Cheema H, George J, Iyer S, Dudeja V, Dawra R, Saluja AK. Extracellular

473   release of ATP promotes systemic inflammation during acute pancreatitis. Am J Physiol

474   Gastrointest Liver Physiol **2019**; 317:G463-G75.

475   49. Csóka B, Németh ZH, Törő G, et al. CD39 improves survival in microbial sepsis by

476   attenuating systemic inflammation. FASEB J **2015**; 29:25-36.

477   50. Aeffner F, Bratasz A, Flaño E, Powell KA, Davis IC. Postinfection A77-1726 treatment

478   improves cardiopulmonary function in H1N1 influenza-infected mice. Am J Respir Cell

479   Mol Biol **2012**; 47:543-51.

480

481

482

FIGURE LEGENDS
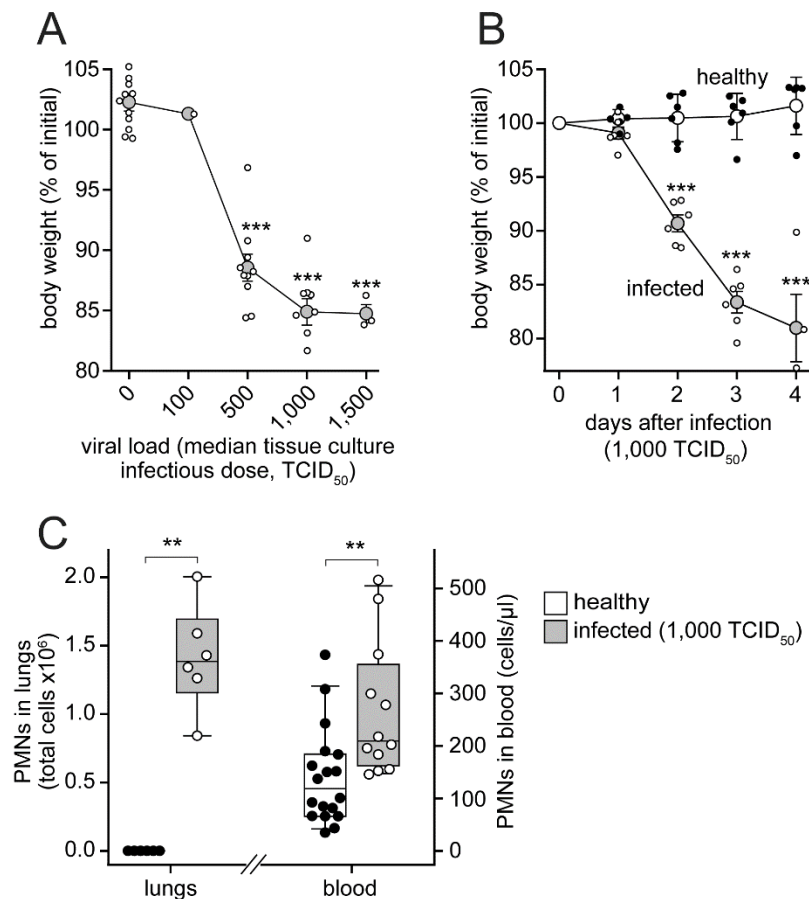
Figure 1. Influenza infection causes dose-and time-dependent weight loss and massive PMN

infiltration of the lungs. A: C57BL/6J mice were intranasally infected with the indicated doses

of PR8 influenza virus and body weight was measured after 3 days. Data are shown as mean ±

SEM (larger circles). In panels A and B, smaller circles indicate results from individual mice;

***p<0.001 vs. uninfected controls, one-way ANOVA. **B:** Mice were infected with 1,000

$TCID_{50}$ of PR8 virus. Body weight was measured daily and compared to the weight of uninfected

litter mates. Data are shown as mean ± SEM; ***p<0.001 vs. uninfected controls, t test. **C:** PMN

numbers in bronchoalveolar lavage fluid (BALF) and in blood were determined 3 days after

infection with 1,000 $TCID_{50}$ of PR8 virus and compared with healthy controls; **p<0.01, Mann-

Whitney test.
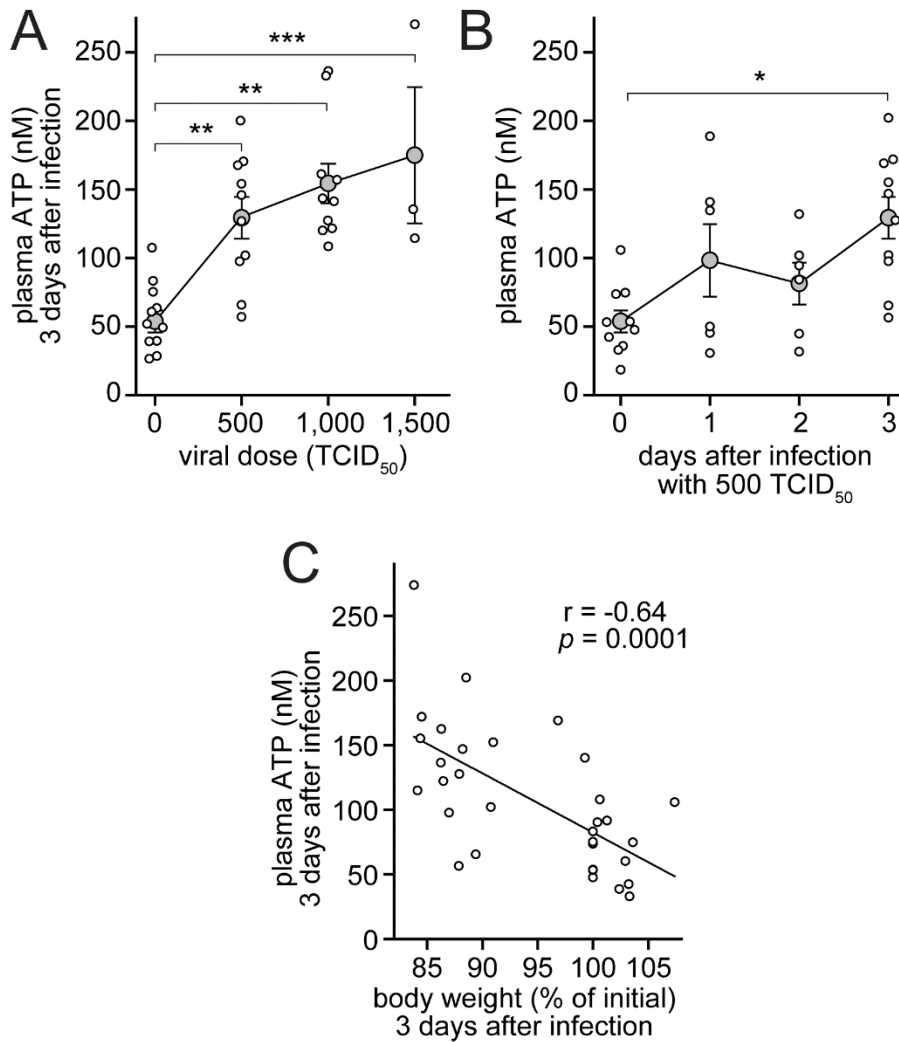
Figure 2. Influenza elevates plasma ATP levels. A: Mice were infected with the indicated doses of PR8 influenza virus and plasma ATP levels were measured 3 days after infection. Results are shown as mean $\pm$ SEM (larger circles). Smaller circles in all panels indicate results from individual mice; ***$p<0.001$, **$p<0.01$, one-way ANOVA. **B:** Mice were infected with 500 $TCID_{50}$ of PR8 virus and ATP plasma levels were measured at indicated time points. Results are shown as mean $\pm$ SEM; *$p<0.05$, Kruskal-Wallis test. **C:** Mice (n=30) were infected with 10-1500 $TCID_{50}$ of PR8 virus and ATP plasma levels and changes in body weight were determined 3 days later; r: Pearson's correlation coefficient.

24

503
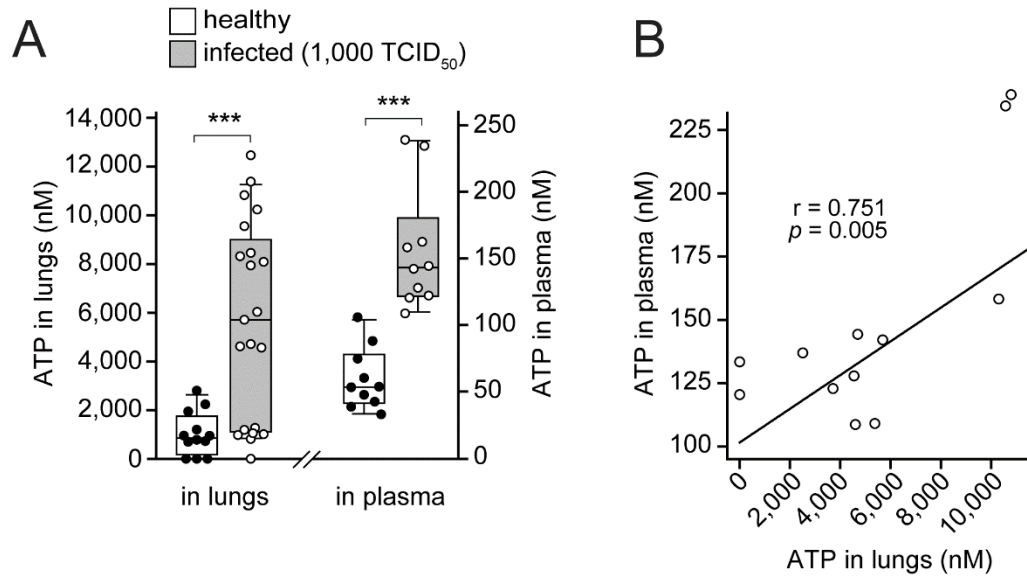
Figure 3. Increased ATP release in the lungs of influenza-infected mice correlates with elevated plasma ATP levels. A: Mice were intranasally treated with PR8 virus (1,000 $TCID_{50}$) or PBS (uninfected controls) and concentrations of ATP in BALF (left) and plasma (right) were measured after 3 days. Circles indicate results from individual mice; ***p<0.001, Mann-Whitney test. **B:** Correlation between ATP levels in plasma and alveolar fluid; r: Pearson's correlation coefficient.

510

511
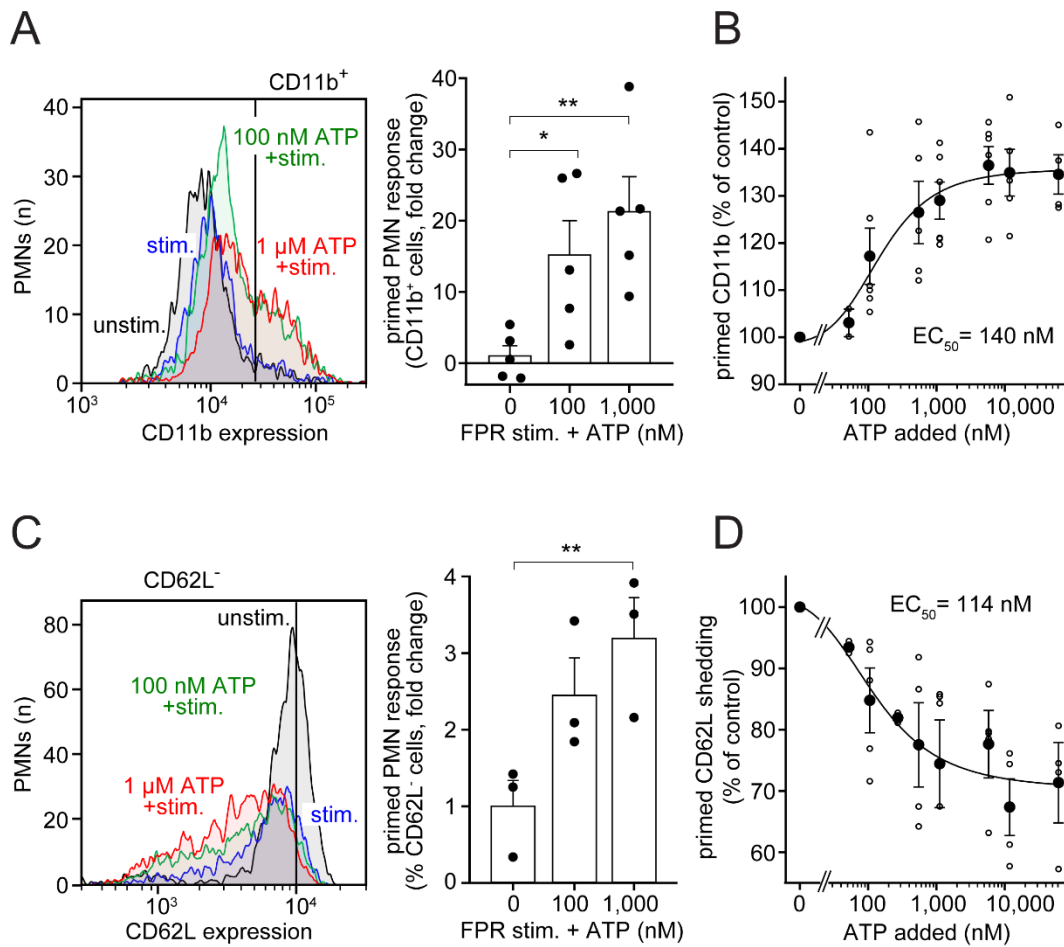
Figure 4. Extracellular ATP primes FPR-stimulated functions of mouse PMNs. Blood

samples from healthy mice were treated with the indicated concentrations of ATP and stimulated

with 50 nM W-peptide for 10 min and CD11b expression (**A-B**) and CD62L shedding (**B-C**)

were analyzed by flow cytometry. Representative histograms and means ± SEM are shown.

Smaller circles are data obtained with individual animals; *p<0.05, **p<0.01 vs. no ATP, one-

way ANOVA; EC_{50}: half maximum effective concentration; FPR: formyl peptide receptor.

518
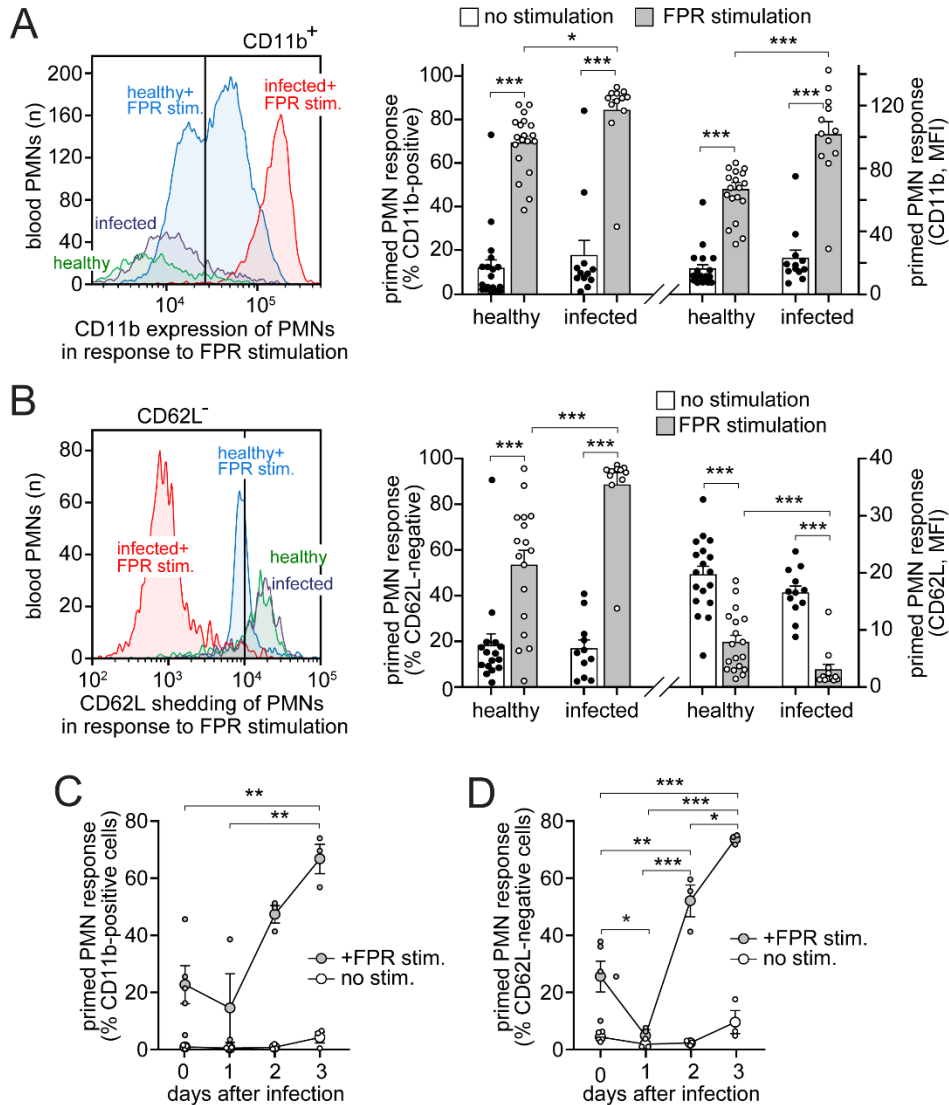
Figure 5. Influenza infection primes blood PMNs. Mice received PR8 influenza virus (1,000

TCID$_{50}$) or PBS (healthy control) and blood samples were collected 3 days later (**A**-**B**) or at the

indicated time points (**C**-**D**) and treated or not (unstimulated controls) with 100 nM W-peptide

for 10 min. CD11b surface expression (**A**, **C**) and CD62L shedding (**B**, **D**) were analyzed by

flow cytometry. Representative histograms and gating of PMN populations are shown in **A** and

B. Data are shown as mean ± SEM of at least 3 independent experiments. Circles indicate results

from individual mice; *p<0.05, **p<0.01, ***p<0.001, one-way ANOVA. FPR: formyl peptide

receptor; MFI: mean fluorescence intensity.
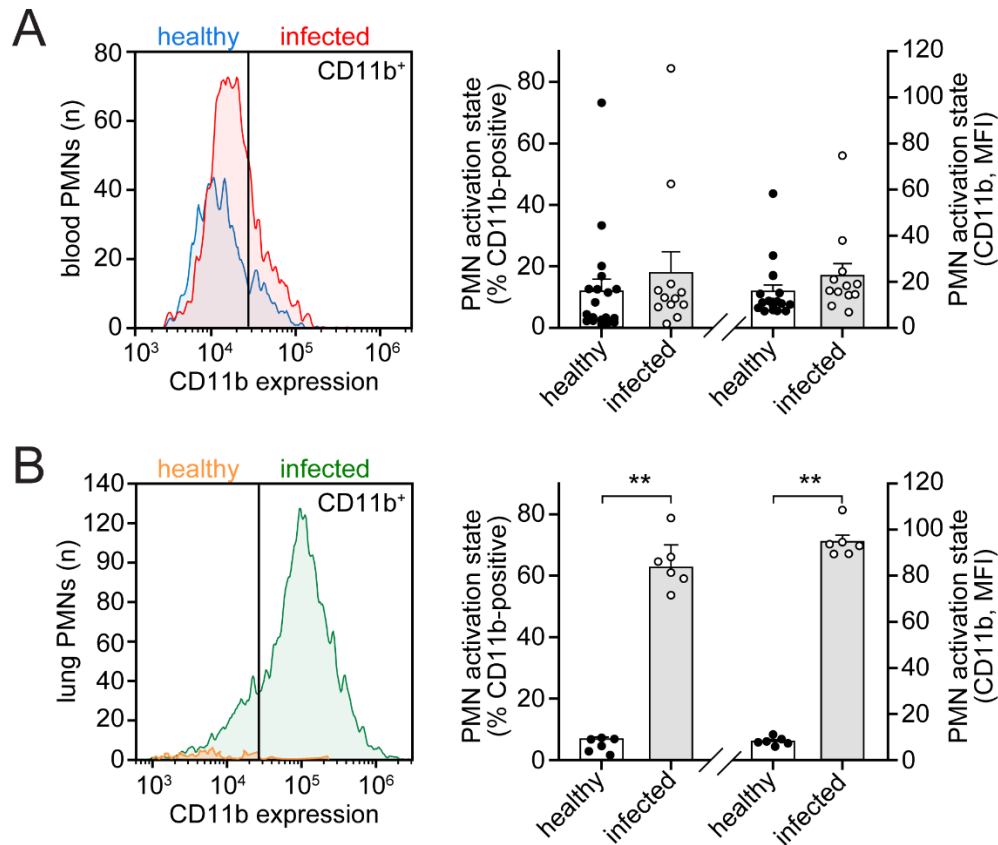
Figure 6. Influenza virus infection activates PMNs only after their recruitment to the lungs.
Mice were intranasally infected with PR8 influenza virus (1,000 $TCID_{50}$) or PBS (healthy
controls) and blood and BALF samples were collected 3 days later. CD11b surface expression on
PMNs in blood (**A**) or lungs (**B**) was analyzed by flow cytometry. Representative histograms and
averaged results (mean ± SEM) of at least 3 separate experiments are shown. Circles indicate
results from individual mice; **p=0.002, Mann-Whitney test; MFI: mean fluorescence intensity.
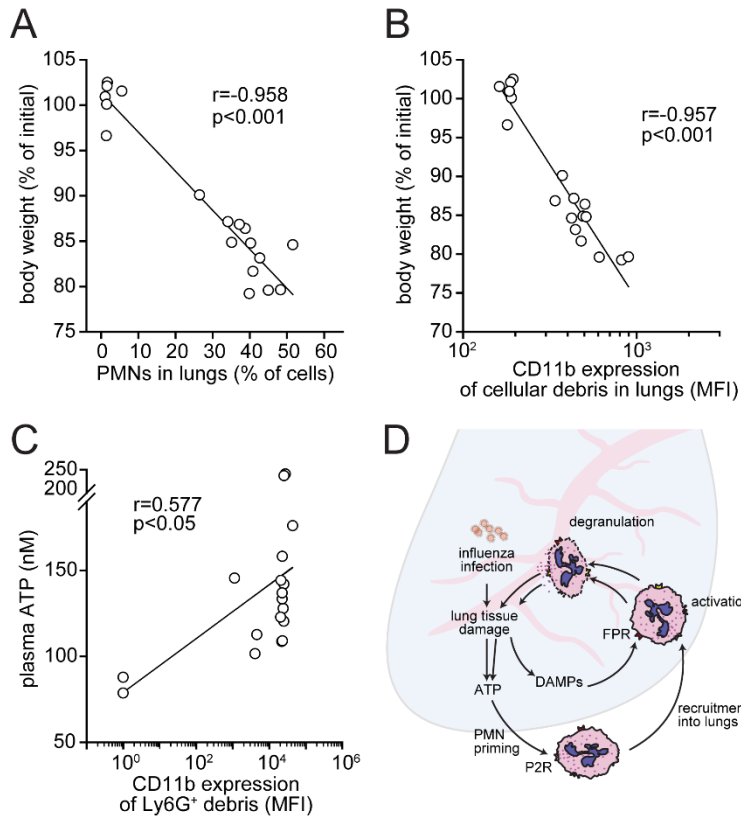
Figure 7. PMN influx correlates with disease progression. A-C: Mice received PR8 influenza

virus (1,000 $TCID_{50}$; n=12) or PBS (healthy controls; n=6) and BALF samples were collected 3

days later. Samples were stained with anti-CD11b and anti-Ly6G antibodies. The percentage of

PMNs (**A**) and cellular debris expressing CD11b (**B**, **C**) were analyzed by flow cytometry and

correlated with body weight loss and ATP plasma levels. **D:** Proposed model of ATP-induced

PMN priming and activation in influenza disease progression. Influenza-associated tissue

damage releases ATP and other damage-associated molecular patterns (DAMPs) into the

extracellular space. Systemic spread of ATP primes PMNs by triggering their P2 receptors

(P2R). Local stimulation of primed PMNs in the lungs by FPR and DAMPs causes excessive

PMN activation, degranulation, and tissue damage that promotes disease progression. FPR:

formyl peptide receptor; MFI: mean fluorescence intensity
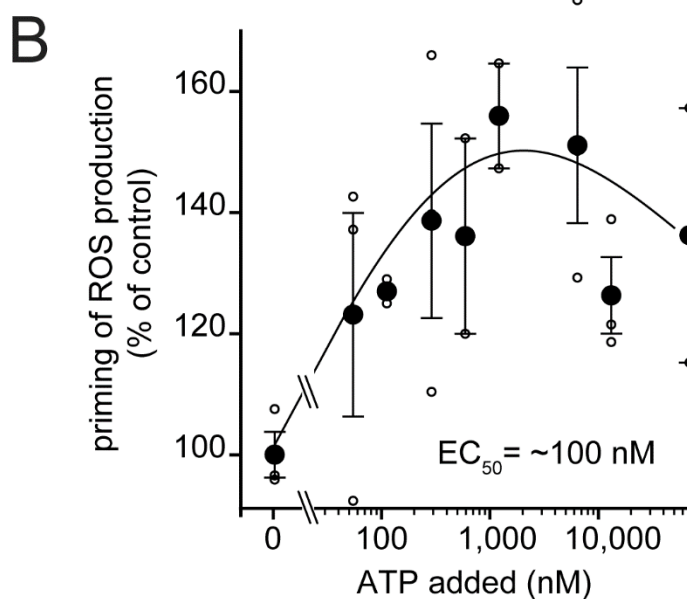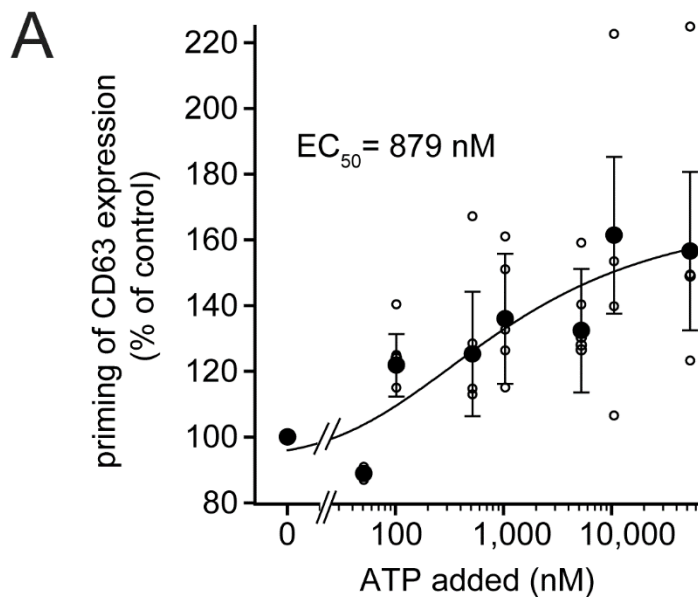
Supplementary Figure 1. Extracellular ATP primes degranulation and superoxide production of FPR-stimulated mouse PMNs. Blood samples from healthy mice were stimulated with W-peptide in the presence or absence of the indicated ATP concentrations and CD63 expression (**A**) and reactive oxygen species (ROS) production (**B**) were analyzed by flow cytometry. Results are shown as means ± SEM (n≥3 different mice); *p<0.05, **p<0.01 vs. 0 nM ATP added; one-way ANOVA; EC50: half maximum effective concentration.